Enhanced Trans-Himalaya Pollution Transport to the Tibetan Plateau by the Cut-off Low System

Ruixiong Zhang[1], Yuhang Wang[1], Qiusheng He[2], Laiguo Chen[3], Yuzhong Zhang[1], Hang Qu[1], Charles Smeltzer[1], Jianfeng Li[1], Leonardo M.A. Alvarado[4], Mihalis Vrekoussis[4,5,6], Andreas Richter[4], Folkard Wittrock[4], and John P. Burrows[4]

[1]School of Earth and Atmospheric Sciences, Georgia Institute of Technology, Atlanta, GA
[2]School of Environment and Safety, Taiyuan University of Science and Technology, Taiyuan, China
[3]Urban Environment and Ecology Research Center, South China Institute of Environmental Sciences (SCIES), Ministry of Environmental Protection (MEP), Guangzhou, China
[4] Institute of Environmental Physics and Remote Sensing, University of Bremen, Bremen, Germany
[5] Center of Marine Environmental Sciences – MARUM, University of Bremen, Germany
[6] Energy, Environment and Water Research Center (EEWRC), The Cyprus Institute, Nicosia, Cyprus

Correspondence to: Yuhang Wang (ywang@eas.gatech.edu), Qiusheng He (heqs@tyust.edu.cn)

Abstract. Long-range transport and subsequent deposition of black carbon on glaciers of Tibet is one of the key issues of climate research inducing changes on radiative forcing and subsequently impacting on the melting of glaciers. The transport mechanism, however, is not well understood. In this study, we use short-lived reactive aromatics as proxies to diagnose transport of pollutants to Tibet. In situ observations of short-lived reactive aromatics across the Tibetan Plateau are analyzed using a regional chemistry and transport model. The model performance using the current emission inventories over the region is poor due to problems in the inventories and model transport. Top-down emissions constrained by satellite observations of glyoxal (CHOCHO) are a factor of 2-6 higher than the a priori emissions over the industrialized Indo-Gangetic Plain. Using the top-down emissions, agreement between model simulations and surface observations of aromatics improves. We find enhancements of reactive aromatics over Tibet by a factor of 6 on average due to rapid transport from India and nearby regions during the presence of a high-altitude cut-off low system. Our results suggest that the cut-off low system is a major pathway for long-range transport of pollutants such as black carbon. The modeling analysis reveals that even the state-of-the-science high-resolution reanalysis cannot simulate this cut-off low system accurately, which probably explains in part the underestimation of black carbon deposition over Tibet in previous modeling studies. Furthermore, another model deficiency of underestimating pollution transport from the south is due to the complexity of terrain, leading to enhanced transport. It is therefore challenging for coarse-resolution global climate models to properly represent the effects of long-range transport of pollutants on the Tibetan environment and the subsequent consequence for regional climate forcing.

Atmospheric
Chemistry
and Physics
Discussions

1 Introduction

The Tibetan Plateau, commonly referred as the Third Pole and the last pristine land of the Earth, has drawn much attention in environmental and climate research in recent years. Although Tibet appears to be isolated from industrialized regions due in part to the transport barrier by its being a plateau and its pollutant concentrations being generally low, the Third Pole is vulnerable to regional climate change. Areas of the Tibetan Plateau over 4 km are warming at a rate of 0.3 °C per decade, twice as fast as the global average (Xu et al., 2009). In addition to the increase of greenhouse gases (GHGs) and the associated global warming, black carbon (BC) is likely another important contributor to the warming of the Tibetan Plateau. The deposition of BC on the vast glaciers of the Tibetan Plateau will decrease the surface albedo, accompanied by increased sunlight absorption and subsequent enhanced melting (Hansen and Nazarenko, 2004; Ramanathan and Carmichael, 2008; Ming et al., 2009). The dwindling of glaciers over Tibet is a major concern for fresh water supply to a large portion of the Asian population through the Indus River, Ganges River, Yarlung Tsangpo River, Yangtze River and Yellow River (Singh and Bengtsson, 2004; Barnett et al., 2005; Lutz et al., 2014). Though melting glaciers favor river runoff temporarily, mass loss of glaciers endangers water supply during the dry season in the future (Yao et al., 2004; Kehrwald et al., 2008).

Increasing BC concentrations were already found in ice core and lake sediment records (Xu et al., 2009; Cong et al., 2013). Besides narrowing the uncertainties of BC emissions, aging and deposition, better understanding the transport pathways are equally important in this region. Surrounded by the largest black carbon sources of East Asia and South Asia (Bond et al., 2007; Ohara et al., 2007), Tibet is affected by pollutant transport from these two regions (Kopacz et al., 2011; Lu et al., 2012; Wang et al., 2015; Zhang et al., 2015). Hindman and Upadhyay (2002) proposed that the vertical lifting due to convection and subsequent horizontal mountain-valley wind lead to the transport of condensation nuclei from Nepal to Tibet. Cong et al. (2015) suggested that both the large-scale westerlies from East Asia and the local mountain-valley wind from South Asia are major transport pathways. Observation-constrained modeling, however, is needed to better understand potential model biases.

In this study, we use short-lived reactive aromatics as proxies to diagnose transport of pollutants to Tibet. In situ observations of short-lived reactive aromatics across the Tibetan Plateau are analyzed (Section 2.1). Anthropogenic emissions including fossil fuel combustion, gasoline evaporation and solvent use constitute the main source of atmospheric aromatics (Sack et al., 1992; Fu et al., 2008; Henze et al., 2008; Cagliari et al., 2010; Cabrera-Perez et al., 2016). Biofuel and biomass burning is another important source (Fu et al., 2008; Henze et al., 2008). The main sink of aromatics is OH oxidation with lifetimes ranging from hours to days (Atkinson 2000; Liu et al., 2012b). We use satellite observations to minimize the biases of emission inventories for upwind regions of Tibet (Sections 2.2, 2.3 and 2.4) and then apply a regional chemistry and transport model constrained by high-resolution reanalysis meteorological data to understand missing transport processes in model simulations (Section 3). On the basis of these results, we examine the implications for global climate modeling studies of anthropogenically driven changes over the Tibetan Plateau (Section 4).

Atmospheric
Chemistry
and Physics
Discussions

Open Access

EGU

2 Methods

2.1 In situ aromatics data

Whole air samples were collected in 2-L electro-polished stainless-steel canisters, which had been cleaned and vacuumed according to the TO-15 method issued by US EPA before shipment to the sampling sites. The restricted grab sampler (39-RS-x; Entech), which has a 5-µm Silonite-coated metal particulate filter, was placed on the inlet of the canister to completely filter out dust and other particulates during sampling. These samples were taken in daytime from 8:00 AM to 7:00 PM with an interval of 1 to 2 hours. The sampling time was 5 minutes to fill the vacuumed canisters. The filled canisters were transported back to the laboratory of Guangzhou Institute of Geochemistry, Chinese Academy of Science. Each air sample was analyzed for 65 light non-methane hydrocarbons (NMHCs) species. The samples were pretreated by an Entech Model 7100 Preconcentrator (Entech Instruments Inc., California, USA), and analyzed by a gas chromatography-mass selective detector (GC-MSD/FID, Agilent 7890A/5973N, USA) using dual columns and dual detectors to simultaneously analyze both low- and high-boiling-point VOCs with each injection. The detailed analytical procedure is described by Zhang et al. (2012).

In this study, we analyze 65 measurements of aromatics (benzene, toluene, ethyl-benzene, m/p/o-xylene) and wind speed measurements taken across Tibet during October 2010 (Fig. 1b). Care was taken in sampling such that there are no direct urban, industrial, or road emissions in the upwind direction of the sampling location. The lifetimes of toluene, ethyl-benzene, m/p/o-xylene are relatively short (2-20 hours) and these reactive aromatic compounds therefore provide observational constraints for transport from India and nearby regions to Tibet. We group the samples into three periods based on the time and locations of the measurements, i.e. Period 1 from October 13 to 17, 2010 to the north of the Himalayas along the southern border of Tibet, Period 2 from October 19 to 24 across the interior of the Tibetan Plateau, and Period 3 of October 25 to the West of the Yarlung Tsangpo Grand Canyon in southeastern Tibet (Fig. 1b).

2.2 SCIAMACHY CHOCHO measurements

The SCanning Imaging Absorption spectroMeter for Atmospheric CHartographY (SCIAMACHY) onboard Environmental Satellite (ENVISAT) operated from 2002 to 2012 (Burrows et al., 1995, Bovensmann et al., 1999), with an overpassing time at about 10:00 AM local time. SCIAMACHY made passive remote sensing measurements of the upwelling radiation from the top of the atmosphere in alternate nadir and limb viewing geometry. Mathematical inversion of the measurements of SCIAMACHY yields a variety of data products including glyoxal (CHOCHO) Vertical Column Densities (VCDs, unit: $molecules\ cm^{-2}$). The retrieval uses the Differential Optical Absorption Spectroscopy (DOAS) technique (Wittrock et al., 2006; Vrekoussis et al., 2009; Alvarado et al., 2014). The CHOCHO retrieval used in this study is based on the algorithm developed in Alvarado et al. (2014), which includes corrections for the interferences with nitrogen dioxide (NO$_2$) over the regions with high NOx emissions as well as liquid water over oceans (Alvarado, 2016). Detection limit for SCIAMACHY CHOCHO VCD is about $1 \times 10^{14}\ molecules\ cm^{-2}$. The overall monthly uncertainty of CHOCHO VCDs ($C_{CHOCHO}^{observed}$) in the selected region during October 2010 is given by $\alpha \times C_{CHOCHO}^{observed} + 1 \times 10^{14}\ molecules\ cm^{-2}$, where the value of α is in a

range of 0.1 to 0.3. Following the method as described by Liu et al. (2012b), we derive a top-down aromatics emission estimate for South Asia constrained by CHOCHO retrievals described in Section 2.4.

2.3 3-D REAM model

We use the 3-D Regional chEmical trAnsport Model (REAM) to examine the chemistry evolution and regional transport of

5   aromatics. REAM was used in previous studies, including large-scale transport (Wang et al., 2006; Zhao et al., 2009b, 2010), vertical transport (Zhao et al., 2009a; Zhang et al., 2014, 2016), emission estimates (Zhao and Wang, 2009; Liu et al., 2012b; Gu et al., 2013, 2014) and other air quality studies (Zeng et al., 2003, 2006; Choi et al., 2005, 2008a, 2008b; Wang et al., 2007; Liu et al.,2010, 2012a, 2014; Gray et al., 2011; Yang et al., 2011; Zhang and Wang, 2016).

REAM has a horizontal resolution of 36 km with 30 vertical levels in the troposphere covering adjacent regions of China (Fig.

10   1a). The WRF domain is larger than that of REAM by 10 grid cells on each side. The recent update of REAM expands the GEOS-Chem standard chemical mechanism (V9-02) to include a detailed description of aromatic chemistry (Liu et al., 2010, 2012b). Aromatics are lumped into three species based on reactivity, i.e. ARO1 (toluene, ethyl-benzene), ARO2 (m/p/o-xylene), and benzene. The atmospheric lifetimes of the three aromatics tracers against OH are 18 hours, 4.2 hours and 3.9 days during the study period (October 13-25, 2010), respectively. Due to the long atmospheric lifetime of benzene, it is more

15   difficult to track and identify its sources; thus we do not explicitly discuss benzene in this study. We focus our analysis on reactive aromatics (toluene, ethyl-benzene, and m/p/o-xylene).

Meteorological fields in REAM are obtained from the Weather Research and Forecasting model (WRF) assimilation constrained by National Centers for Environmental Prediction Climate Forecast System Reanalysis (NCEP CFSR, Saha et al., 2010). CFSR has a horizontal resolution of T382 (~38 km). Initial and boundary conditions are taken from GEOS-Chem 2° ×

20   2.5° simulation. Anthropogenic emissions in China and other Asian countries are from the Multi-resolution Emission Inventory for China (MEIC v1.0) for 2010 and updated Intercontinental Chemical Transport Experiment-Phase B (INTEX-B) emission for 2006 (Li et al., 2014), respectively. Biogenic VOC emissions are computed with the Model of Emissions of Gases and Aerosols from Nature (MEGAN) algorithm (v2.1, Guenther et al., 2012) and biomass burning emissions of CHOCHO and other species are based on Global Fire Emissions Database Version 4.1 with small fires (GFED4.1s, van der

25   Werf et al., 2010; Andreae and Merlet, 2001; Lerot et al., 2010).

We updated the INTEX-b emission inventory in South Asian countries through inverse modeling constrained by SCIAMACHY CHOCHO VCDs (Section 2.4). We run REAM simulations with the a priori and top-down emission inventories, and compare the results with observations in Section 3.1 and 3.2, respectively. We find that some of the model low bias is likely due to emission underestimation. We further carried out three model sensitivity tests to calculate the contributions to

30   surface aromatics from emissions over Tibet, other provinces of China, and South Asia (India and nearby regions). Each simulation is run with only the aromatics emissions from the corresponding region. The results for two sub-periods of Period 2 are examined in Section 3.3.

Atmospheric
Chemistry
and Physics
Discussions

2.4 Top-down aromatics emission estimation

Compared with SCIAMACHY data, REAM using the original emission inventories archived at the overpassing time of SCIAMACHY underestimates CHOCHO VCDs in the populated regions of India (Fig. 2), especially the Indo-Gangetic Plain located south of the Himalayas. We then derive the top-down aromatics emissions for these regions constrained by

5   SCIAMACHY CHOCHO data (Liu et al., 2012b; Alvarado, 2016).

First, we calculate the difference between observed ($C_{CHOCHO}^{SCIAMACHY}$, Fig. 2a) and modeled (C_{CHOCHO}^{REAM}, Fig. 2b) CHOCHO VCDs with original emissions ($\Delta C_{CHOCHO} = C_{CHOCHO}^{SCIAMACHY} - C_{CHOCHO}^{REAM}$, Fig. S2a in Supplement). We then discuss the potential reasons for the difference, i.e. primary emissions from biomass burning and secondary sources from isoprene, acetylene, ethylene and aromatics.

10   Biomass burning is often a major primary source of CHOCHO (Myriokefalitakis et al., 2008). GFED4.1s inventories, as well as fire hotspots observed by MODIS on board the Terra and Aqua satellites, indicate only a small number of fire occurrences during this period in South Asia, with the exception of crop residue burning in Punjab, an agricultural state in North India. The distribution of localized CHOCHO emissions from biomass burning (Fig. S1 in Supplement) differs greatly from that of ΔC_{CHOCHO} (Fig. S2a in Supplement), which is large over the industrialized Indo-Gangetic Plain. Therefore, it is considered that

15   the large model underestimation of CHOCHO over the Indo-Gangetic Plain is unlikely due to biomass burning.

Direct anthropogenic emissions of CHOCHO are small (Volkamer et al., 2005; Stavrakou et al., 2009; Liu et al., 2012 b). CHOCHO is produced primarily from the photochemical oxidation of biogenic compounds (e.g., isoprene and terpenes) and hydrocarbon released by anthropogenic activities (e.g., acetylene, ethylene, and aromatics) (Fu et al., 2008). Due to the long atmospheric lifetime of acetylene and ethylene, their contributions to CHOCHO concentrations are quite small in South Asia

20   during October 2010. The most significant secondary sources of CHOCHO in South Asia are isoprene (Fig. S2b in Supplement) and aromatics (Fig. S2c in Supplement). Biogenic isoprene emissions depend on vegetation, sunlight, and temperature. High isoprene emissions are to the southeast of the Indo-Gangetic Plain, where CHOCHO VCDs are high in both the observations and model simulations. In comparison, aromatics oxidation dominates CHOCHO over the Indo-Gangetic Plain, where model underestimation is largest (Fig. 2 and Fig. S2 in Supplement).

25   We apply the approach by Liu et al. (2012b) to estimate the top-down emissions of aromatics based on SCIAMACHY CHOCHO VCDs. As found by Liu et al. (2012b), domain-wide inversion is impractical since model results correlate poorly with gridded satellite data, most likely reflecting the problems in the spatial distribution of a priori emissions. We therefore determine the emissions by inversion for each grid cell at the overpassing time of SCIAMACHY as Liu et al. (2012b) and find similar results for India and nearby regions as Liu et al. (2012b) for eastern China. The top-down biogenic isoprene emissions

30   are essentially the same as the a priori emissions. However, the top-down anthropogenic emissions of aromatics (Fig. S3b in Supplement) increase by a factor of 2-6. The improved model comparison with in situ observations will be discussed in the next section. One caveat with respect to the top-down emission estimate is that we have to assume that the speciation of aromatics in the a priori emission inventory is correct. Since the purpose of this work is to study transport pathways to the

Tibetan Plateau on the basis of in situ observations, we examine lumped reactive aromatics (defined as the sum of toluene, ethyl-benzene, and m/p/o-xylene) in the model evaluation (Section 3.2). Satellite observations cannot be used for this purpose since CHOCHO VCDs over Tibet are below or around the detection limit.

3 Results and discussion

3.1 Observed and simulated reactive aromatics

The average of observed reactive aromatics surface concentration (59±63 pptv) over the Tibetan Plateau is considerably lower than the values found for megacities of China, such as Beijing (8.04 ppbv) and Shanghai (5.2 ppbv) (Liu et al., 2012b). Higher aromatics levels were measured during Period 1 (76±39 pptv) and Period 3 (169±57 pptv) than in Period 2 (26±39 pptv). The model simulation using the a priori emissions in general compares poorly with the in situ observations (Fig. 3). The best performance is during the low-concentration Period 2 when the model underestimates the observations by about a factor of 2. However, the relatively high correlation coefficient (R^2=0.88) suggests that atmospheric transport and emission distribution are reasonably simulated. This is in sharp contrast to Periods 1 and 3 when the model underestimates the observations by a factor of 5-7 with no or very low correlations between model and the observations (slope=0.24 and 0.15, R^2=0.00 and 0.02 for Period 1 and 3, respectively). We discuss the different reasons for the model performance for Period 1, 2 and 3 in the next 3 sections.

3.2 Improvements due to top-down emissions

Fig. 2 and Fig. S3 in Supplement show that SCIAMACHY observations of CHOCHO suggest much higher industrial emissions of aromatics over the Indo-Gangetic Plain than the a priori emissions. We derive top-down emissions on the basis of SCIAMACHY CHOCHO VCDs (Section 2.4). Top-down emissions are higher than the a priori emissions by a factor of 2-6 over the Indo-Gangetic Plain, which is the upwind region of the Tibetan Plateau. Fig. 4 shows the resulting improvement in the model simulation. The large underestimations of CHOCHO VCDS over the Indo-Gangetic Plain are corrected as expected (Fig. 4a). At the same time, in situ observations during Period 2 are much better reproduced by the model with the slope increasing from 0.62 to 0.95 and a similar R^2 value (0.80) (Fig. 4b). In contrast, model simulations for Periods 1 and 3 are not improved using top-down emission estimates with low biases similar to the original model simulation. This indicates that the reasons for the discrepancies in Periods 1 and 3 are probably not related to the uncertainties in emissions but could be linked to deficiencies in model transport in this area.

3.3 Rapid trans-Himalaya transport due to a high-level cut-off Low System

Observed and simulated reactive aromatics concentrations show large variability during Period 2 (Fig. 4b). An investigation of these data shows that a major contributor is meteorology. Observed concentrations of reactive aromatics during October 19-20 are generally lower (6.6±3.4 pptv), in comparison to those during October 21-24 (37±45 pptv). The concentration difference

during the two time periods is captured by model simulations with top-down emissions (Fig. 5). Analysis of WRF simulated surface wind speed shows an increase by a factor of 2-4 from October 19-20 (Fig. 5a) to 21-24 (Fig. 5b), corresponding well to increasing transport of aromatics from the Indo-Gangetic Plain.

To further analyze the difference between the two time periods, we conduct sensitivity simulations in which OH concentrations in the model are specified to the archived values of the full model simulation using top-down emissions. We compute the source attributions for emissions over Tibet, India and nearby regions, and China excluding Tibet (Fig. 6). During October 19-20, reactive aromatics are due to Tibetan emissions. With the exception of one data point, concentrations are ≤ 7 pptv. On October 21, emissions from India and nearby regions become dominant while the concentrations are still low (7-18 pptv). During October 22-24, however, emissions from India and nearby regions contribute much higher concentrations (12-128 pptv). The only exception is one data point sampled at 30 km east of Lhasa, where most of the population of Tibet resides. The contribution by emissions of India and nearby regions to this data point is ~20 pptv, still much higher than during October 19-20. The contribution by emissions from China (excluding Tibet) is negligible (~1%) for this period.

The rise of the Tibetan Plateau is a natural barrier for pollution transport (Fig. 1). Considering the high altitude of the Tibetan Plateau, we analyze 300 hPa geopotential height field in order to understand the change of wind circulation over the region (Fig. 5). During October 19-20, the upper troposphere shows a northward gradual pressure decrease, which does not provide near-surface forcing of trans-Himalaya transport (Fig. 5a). During October 21-24, the presence of a southeastward-moving upper tropospheric cut-off low system induces increasingly stronger surface wind from India to Tibet (Fig. 5b, Hoskins et al., 1985). Trans-Himalaya air mass flux in the lower atmosphere shows an increase by a factor of 2 to 5 (Fig. S4 in Supplement). Accompanying this transport, large amounts of pollutants such as reactive aromatics analyzed here are transported to the Tibetan Plateau leading to much higher surface concentrations. Our analysis implies that BC transported in the presence of an upper tropospheric cut-off low is potentially a major contributor to BC deposition to Tibetan glaciers.

3.4 Missing cut-off low system and complex terrain

Compared to Period 2, model performance for Periods 1 and 3 is very poor with severe low biases (Fig. 3). Transport deficiency appears to be the main problem. Fig. 7 shows the histograms of observed and simulated wind speed for the 3 periods. The observed and simulated wind speed distributions are similar for Period 2 (Fig. 7c). In comparison, the simulated wind speed distribution differs drastically for the other two periods (Fig. 7a and 7d).

The wind speed distributions are more similar between Period 1 and 2 in the observations than model simulations. The underestimation of wind speed in Period 1 leads to slower transport of pollutants from the Indo-Gangetic Plain and consequently to a low bias in surface reactive aromatics in the model. Examination of the 300 hPa geopotential height field during October 13-17 of Period 1 shows a weak trough northeast of Kazakhstan in CSFR reanalysis and WRF simulation results (Fig. S5 in Supplement). A strong upper tropospheric low pressure system, akin to the cut-off low system of Fig. 5b, will induce stronger lower troposphere wind circulation. The lack of radiosonde observations over the interior of the Tibetan Plateau to constrain the meteorological reanalysis is the plausible reason (Fig. S6 in Supplement). The horizontal scale of the

Rossby Wave at northern mid latitudes is thousands of kilometers, which can be reasonably represented by the density of the existing radiosonde network. We hypothesize that the smaller scale cut-off low system, not simulated in reanalysis, is more likely the reason for the model-observation discrepancy during Period 1. We resample surface wind speed of October 23, when a cut-off low system leads to rapid trans-Himalaya transport in Period 2 analyzed in the previous section. At the same time of

5   the day and location as the observations, the simulated wind speed histogram is in good agreement with the observations (Fig. 7b). The corresponding air mass flux across the Himalayas would have been much stronger in the presence of a cut-off low system (Fig. S7 in Supplement).

During Period 3, the observed wind speed histogram is skewed to very low wind speed (0-1 m/s) compared to the simulations (Fig. 7d). Sampling bias to avoid locations with strong wind is a possible reason. Another reason is that these samples were

10   taken at lower altitudes in valleys compared to higher altitudes in the other two periods. Inspection of Fig. 1 shows the complex terrain surrounding the valleys of Period 3 sampling. Using high-resolution (~ 1 km) terrain data from the U.S. Geological Survey (USGS) Global 30 Arc-Second Elevation (GTOPO30) dataset, we find that the standard deviation of altitude in the $7km \times 7km$ region centered at the corresponding observation location correlates well with the observed reactive aromatics with a R^2 value of 0.55 (Fig. 8), which suggests that pollution transport is strongly enhanced by the effects of complex terrain.

15   The horizontal resolution of 36 km used in this study is inadequate to simulate this effect. Model resolution as high as 1 km appears to be necessary to capture the observed feature but the computational resource requirement will be exceptionally large for a global model such as that used for CFSR. The effects of complex terrain may have also affected the observations of Periods 1 and 2 but to a smaller extent since the terrain variation is lower and sampling altitude is higher in those periods.

4. Conclusions and implications for climate studies

20   We apply the REAM model to analyze in situ observations of reactive aromatics across the Tibetan Plateau. Top-down estimate using SCIAMACHY CHOCHO observations suggests that the a priori inventory for aromatics emissions is low by a factor of 2 to 6 over the industrialized Indo-Gangetic Plain. Application of the top-down emission estimate greatly reduces the low bias of the model during Period 2. Model results suggest that the second half of Period 2 is characterized by rapid trans-Himalaya transport from India and nearby regions driven by the presence of a cut-off low system in the upper troposphere.

25   Model performance for Periods 1 and 3 is poor compared to Period 2 and employing top-down emission estimates does not significantly improve the model simulation of these periods. In situ observations show much stronger surface wind than simulated in the model during Period 1. The lack of radiosonde observations in the interior of the Tibetan Plateau is likely the reason that a cut-off low system, the scale of which is much less than the mid-latitude Rossby wave, is not simulated by the T382 (~38 km) CSFR reanalysis. Consequently, trans-Himalaya transport is greatly underestimated in the model. Sampling of

30   Period 3 is in valleys surrounded by complex terrain. Although observed surface wind is weak, we find that reactive aromatics concentrations are strongly correlated with the complexity of surrounding terrain, implying enhanced pollution transport by terrain driven mixing. Model simulations at a resolution of 36 km are inadequate for simulating the terrain effect.

Atmospheric
Chemistry
and Physics
Discussions

Open Access

EGU

The height of the Tibetan Plateau is a natural barrier for pollution transport into this pristine region. This geographical feature is also a challenge for regional and global model simulations. In this study, we use short-lived reactive aromatics as proxies to evaluate model simulated transport to the Tibetan Plateau on the basis of in situ observations. After correcting for the emission underestimation using satellite observations, simulated trans-Himalaya transport of proxy species (using WRF assimilated

5   meteorological fields) still has significant low biases for two reasons, (1) poor representation of a cut-off low system, and (2) inadequate representation of terrain effect due to a coarse model resolution. These two transport-related issues likely exist in global climate models; the coarser resolution of climate models than our simulations or CSFR may further worsen the transport biases. Our analysis results imply that pollution transport to the Tibetan Plateau, such as BC, is likely to be greatly underestimated in climate models, which was found previously (e.g., He et al., 2014). Further analysis of reanalysis and

10   climate model simulations is required to quantify potential model biases and the resulting effect of simulated BC deposition to glaciers on the Tibetan Plateau due to the transport issues we identified in this study.

Atmospheric
Chemistry
and Physics
Discussions

10 **References**

Alvarado, L. M. A., Richter, A., Vrekoussis, M., Wittrock, F., Hilboll, A., Schreier, S. F., and Burrows, J. P.: An improved glyoxal retrieval from OMI measurements, Atmos. Meas. Tech., 7, 4133-4150, 10.5194/amt-7-4133-2014, 2014.

Alvarado, L. M. A.: Investigating the role of glyoxal using satellite and MAX-DOAS measurements, Ph.D. thesis, University of Bremen, http://elib.suub.uni-bremen.de/edocs/00105347-1.pdf, 2016

15 Andreae, M. O., and Merlet, P.: Emission of trace gases and aerosols from biomass burning, Global Biogeochemical Cycles, 15, 955-966, 10.1029/2000GB001382, 2001.

Atkinson, R.: Atmospheric chemistry of VOCs and NOx, Atmospheric Environment, 34, 2063-2101, http://dx.doi.org/10.1016/S1352-2310(99)00460-4, 2000.

Barnett, T. P., Adam, J. C., and Lettenmaier, D. P.: Potential impacts of a warming climate on water availability in snow-

20 dominated regions, Nature, 438, 303-309, 2005.

Bond, T. C., Bhardwaj, E., Dong, R., Jogani, R., Jung, S., Roden, C., Streets, D. G., and Trautmann, N. M.: Historical emissions of black and organic carbon aerosol from energy-related combustion, 1850–2000, Global Biogeochemical Cycles, 21, n/a-n/a, 10.1029/2006GB002840, 2007.

Bovensmann, H., Burrows, J. P., Buchwitz, M., Frerick, J., Noël, S., Rozanov, V. V., Chance, K. V., and Goede, A. P. H.:

25 SCIAMACHY: Mission Objectives and Measurement Modes, Journal of the Atmospheric Sciences, 56, 127-150, doi:10.1175/1520-0469(1999)056<0127:SMOAMM>2.0.CO;2, 1999.

Burrows, J. P., Hölzle, E., Goede, A. P. H., Visser, H., and Fricke, W.: Earth ObservationSCIAMACHY—scanning imaging absorption spectrometer for atmospheric chartography, Acta Astronautica, 35, 445-451, http://dx.doi.org/10.1016/0094-5765(94)00278-T, 1995.

30 Cabrera-Perez, D., Taraborrelli, D., Sander, R., and Pozzer, A.: Global atmospheric budget of simple monocyclic aromatic compounds, Atmos. Chem. Phys., 16, 6931-6947, 10.5194/acp-16-6931-2016, 2016.

Atmospheric
Chemistry
and Physics
Discussions

Cagliari, J., Fedrizzi, F., Rodrigues Finotti, A., Echevenguá Teixeira, C., and do Nascimento Filho, I.: Volatilization of monoaromatic compounds (benzene, toluene, and xylenes; BTX) from gasoline: Effect of the ethanol, Environmental Toxicology and Chemistry, 29, 808-812, 10.1002/etc.111, 2010.

Choi, Y., Wang, Y., Zeng, T., Martin, R. V., Kurosu, T. P., and Chance, K.: Evidence of lightning NOx and convective transport of pollutants in satellite observations over North America, Geophysical Research Letters, 32, L02805, 10.1029/2004GL021436, 2005.

Choi, Y., Wang, Y., Yang, Q., Cunnold, D., Zeng, T., Shim, C., Luo, M., Eldering, A., Bucsela, E., and Gleason, J.: Spring to summer northward migration of high O3 over the western North Atlantic, Geophysical Research Letters, 35, L04818, 10.1029/2007GL032276, 2008a.

Choi, Y., Wang, Y., Zeng, T., Cunnold, D., Yang, E. S., Martin, R., Chance, K., Thouret, V., and Edgerton, E.: Springtime transitions of NO2, CO, and O-3 over North America: Model evaluation and analysis, J. Geophys. Res.-Atmos., 113, 16, 10.1029/2007jd009632, 2008b.

Cong, Z., Kang, S., Gao, S., Zhang, Y., Li, Q., and Kawamura, K.: Historical Trends of Atmospheric Black Carbon on Tibetan Plateau As Reconstructed from a 150-Year Lake Sediment Record, Environmental Science & Technology, 47, 2579-2586, 10.1021/es3048202, 2013.

Cong, Z., Kawamura, K., Kang, S., and Fu, P.: Penetration of biomass-burning emissions from South Asia through the Himalayas: new insights from atmospheric organic acids, Sci. Rep., 5, 10.1038/srep09580
http://www.nature.com/srep/2015/150330/srep09580/abs/srep09580.html#supplementary-information, 2015.

Fu, T.-M., Jacob, D. J., Wittrock, F., Burrows, J. P., Vrekoussis, M., and Henze, D. K.: Global budgets of atmospheric glyoxal and methylglyoxal, and implications for formation of secondary organic aerosols, Journal of Geophysical Research, 113, 10.1029/2007jd009505, 2008.

Gray, B. A., Wang, Y., Gu, D., Bandy, A., Mauldin, L., Clarke, A., Alexander, B., and Davis, D. D.: Sources, transport, and sinks of SO2 over the equatorial Pacific during the Pacific Atmospheric Sulfur Experiment, Journal of Atmospheric Chemistry, 68, 27-53, 10.1007/s10874-010-9177-7, 2011.

Gu, D., Wang, Y., Smeltzer, C., and Boersma, K. F.: Anthropogenic emissions of NOx over China: Reconciling the difference of inverse modeling results using GOME-2 and OMI measurements, Journal of Geophysical Research: Atmospheres, 119, 2014JD021644, 10.1002/2014JD021644, 2014.

Gu, D. S., Wang, Y. H., Smeltzer, C., and Liu, Z.: Reduction in NOx Emission Trends over China: Regional and Seasonal Variations, Environmental Science & Technology, 47, 12912-12919, 10.1021/es401727e, 2013.

Guenther, A. B., Jiang, X., Heald, C. L., Sakulyanontvittaya, T., Duhl, T., Emmons, L. K., and Wang, X.: The Model of Emissions of Gases and Aerosols from Nature version 2.1 (MEGAN2.1): an extended and updated framework for modeling biogenic emissions, Geosci. Model Dev., 5, 1471-1492, 10.5194/gmd-5-1471-2012, 2012.

Hansen, J., and Nazarenko, L.: Soot climate forcing via snow and ice albedos, Proceedings of the National Academy of Sciences of the United States of America, 101, 423-428, 10.1073/pnas.2237157100, 2004.

He, C., Li, Q. B., Liou, K. N., Zhang, J., Qi, L., Mao, Y., Gao, M., Lu, Z., Streets, D. G., Zhang, Q., Sarin, M. M., and Ram, K.: A global 3-D CTM evaluation of black carbon in the Tibetan Plateau, Atmos. Chem. Phys., 14, 7091-7112, 10.5194/acp-14-7091-2014, 2014.

Henze, D. K., Seinfeld, J. H., Ng, N. L., Kroll, J. H., Fu, T. M., Jacob, D. J., and Heald, C. L.: Global modeling of secondary organic aerosol formation from aromatic hydrocarbons: high- vs. low-yield pathways, Atmos. Chem. Phys., 8, 2405-2420, 10.5194/acp-8-2405-2008, 2008.

Hindman, E. E., and Upadhyay, B. P.: Air pollution transport in the Himalayas of Nepal and Tibet during the 1995–1996 dry season, Atmospheric Environment, 36, 727-739, http://dx.doi.org/10.1016/S1352-2310(01)00495-2, 2002.

Hoskins, B. J., McIntyre, M. E., and Robertson, A. W.: On the use and significance of isentropic potential vorticity maps, Quarterly Journal of the Royal Meteorological Society, 111, 877-946, 10.1002/qj.49711147002, 1985.

Kehrwald, N. M., Thompson, L. G., Tandong, Y., Mosley-Thompson, E., Schotterer, U., Alfimov, V., Beer, J., Eikenberg, J., and Davis, M. E.: Mass loss on Himalayan glacier endangers water resources, Geophysical Research Letters, 35, n/a-n/a, 10.1029/2008GL035556, 2008.

Kopacz, M., Mauzerall, D. L., Wang, J., Leibensperger, E. M., Henze, D. K., and Singh, K.: Origin and radiative forcing of black carbon transported to the Himalayas and Tibetan Plateau, Atmos. Chem. Phys., 11, 2837-2852, 10.5194/acp-11-2837-2011, 2011.

Lerot, C., Stavrakou, T., De Smedt, I., Muller, J. F., and Van Roozendael, M.: Glyoxal vertical columns from GOME-2 backscattered light measurements and comparisons with a global model, Atmospheric Chemistry and Physics, 10, 12059-12072, 10.5194/acp-10-12059-2010, 2010.

Li, M., Zhang, Q., Streets, D. G., He, K. B., Cheng, Y. F., Emmons, L. K., Huo, H., Kang, S. C., Lu, Z., Shao, M., Su, H., Yu, X., and Zhang, Y.: Mapping Asian anthropogenic emissions of non-methane volatile organic compounds to multiple chemical mechanisms, Atmos. Chem. Phys., 14, 5617-5638, 10.5194/acp-14-5617-2014, 2014.

Liu, Z., Wang, Y., Gu, D., Zhao, C., Huey, L. G., Stickel, R., Liao, J., Shao, M., Zhu, T., Zeng, L., Liu, S.-C., Chang, C.-C., Amoroso, A., and Costabile, F.: Evidence of Reactive Aromatics As a Major Source of Peroxy Acetyl Nitrate over China, Environmental Science & Technology, 44, 7017-7022, 10.1021/es1007966, 2010.

Liu, Z., Wang, Y., Gu, D., Zhao, C., Huey, L. G., Stickel, R., Liao, J., Shao, M., Zhu, T., Zeng, L., Amoroso, A., Costabile, F., Chang, C. C., and Liu, S. C.: Summertime photochemistry during CAREBeijing-2007: ROx budgets and O3 formation, Atmos. Chem. Phys., 12, 7737-7752, 10.5194/acp-12-7737-2012, 2012a.

Liu, Z., Wang, Y., Vrekoussis, M., Richter, A., Wittrock, F., Burrows, J. P., Shao, M., Chang, C.-C., Liu, S.-C., Wang, H., and Chen, C.: Exploring the missing source of glyoxal (CHOCHO) over China, Geophysical Research Letters, 39, L10812, 10.1029/2012GL051645, 2012b.

Liu, Z., Wang, Y., Costabile, F., Amoroso, A., Zhao, C., Huey, L. G., Stickel, R., Liao, J., and Zhu, T.: Evidence of Aerosols as a Media for Rapid Daytime HONO Production over China, Environmental Science & Technology, 48, 14386-14391, 10.1021/es504163z, 2014.

Atmospheric
Chemistry
and Physics
Discussions

Lu, Z., Streets, D. G., Zhang, Q., and Wang, S.: A novel back-trajectory analysis of the origin of black carbon transported to the Himalayas and Tibetan Plateau during 1996–2010, Geophysical Research Letters, 39, n/a-n/a, 10.1029/2011GL049903, 2012.

Lutz, A. F., Immerzeel, W. W., Shrestha, A. B., and Bierkens, M. F. P.: Consistent increase in High Asia's runoff due to increasing glacier melt and precipitation, Nature Clim. Change, 4, 587-592, 10.1038/nclimate2237 http://www.nature.com/nclimate/journal/v4/n7/abs/nclimate2237.html#supplementary-information, 2014.

Ming, J., Xiao, C., Cachier, H., Qin, D., Qin, X., Li, Z., and Pu, J.: Black Carbon (BC) in the snow of glaciers in west China and its potential effects on albedos, Atmos. Res., 92, 114-123, http://dx.doi.org/10.1016/j.atmosres.2008.09.007, 2009.

Myriokefalitakis, S., Vrekoussis, M., Tsigaridis, K., Wittrock, F., Richter, A., Brühl, C., Volkamer, R., Burrows, J. P., and Kanakidou, M.: The influence of natural and anthropogenic secondary sources on the glyoxal global distribution, Atmos. Chem. Phys., 8, 4965-4981, 10.5194/acp-8-4965-2008, 2008.

Ohara, T., Akimoto, H., Kurokawa, J.-I., Horii, N., Yamaji, K., Yan, X., and Hayasaka, T.: An Asian emission inventory of anthropogenic emission sources for the period 1980–2020, Atmospheric Chemistry and Physics, 7, 4419-4444, 2007.

Ramanathan, V., and Carmichael, G.: Global and regional climate changes due to black carbon, Nature Geosci, 1, 221-227, 2008.

Sack, T. M., Steele, D. H., Hammerstrom, K., and Remmers, J.: A survey of household products for volatile organic compounds, Atmospheric Environment. Part A. General Topics, 26, 1063-1070, http://dx.doi.org/10.1016/0960-1686(92)90038-M, 1992.

Saha, S., Moorthi, S., Pan, H.-L., Wu, X., Wang, J., Nadiga, S., Tripp, P., Kistler, R., Woollen, J., Behringer, D., Liu, H., Stokes, D., Grumbine, R., Gayno, G., Wang, J., Hou, Y.-T., Chuang, H.-Y., Juang, H.-M. H., Sela, J., Iredell, M., Treadon, R., Kleist, D., Van Delst, P., Keyser, D., Derber, J., Ek, M., Meng, J., Wei, H., Yang, R., Lord, S., Van Den Dool, H., Kumar, A., Wang, W., Long, C., Chelliah, M., Xue, Y., Huang, B., Schemm, J.-K., Ebisuzaki, W., Lin, R., Xie, P., Chen, M., Zhou, S., Higgins, W., Zou, C.-Z., Liu, Q., Chen, Y., Han, Y., Cucurull, L., Reynolds, R. W., Rutledge, G., and Goldberg, M.: The NCEP Climate Forecast System Reanalysis, Bulletin of the American Meteorological Society, 91, 1015-1057, 10.1175/2010BAMS3001.1, 2010.

Singh, P., and Bengtsson, L.: Hydrological sensitivity of a large Himalayan basin to climate change, Hydrological Processes, 18, 2363-2385, 2004.

Stavrakou, T., Muller, J. F., De Smedt, I., Van Roozendael, M., Kanakidou, M., Vrekoussis, M., Wittrock, F., Richter, A., and Burrows, J. P.: The continental source of glyoxal estimated by the synergistic use of spaceborne measurements and inverse modelling, Atmospheric Chemistry and Physics, 9, 8431-8446, 10.5194/acp-9-8431-2009, 2009.

van der Werf, G. R., Randerson, J. T., Giglio, L., Collatz, G. J., Mu, M., Kasibhatla, P. S., Morton, D. C., DeFries, R. S., Jin, Y., and van Leeuwen, T. T.: Global fire emissions and the contribution of deforestation, savanna, forest, agricultural, and peat fires (1997–2009), Atmos. Chem. Phys., 10, 11707-11735, 10.5194/acp-10-11707-2010, 2010.

Volkamer, R., Molina, L. T., Molina, M. J., Shirley, T., and Brune, W. H.: DOAS measurement of glyoxal as an indicator for fast VOC chemistry in urban air, Geophysical Research Letters, 32, n/a-n/a, 10.1029/2005GL022616, 2005.

Atmospheric
Chemistry
and Physics
Discussions

Open Access

EGU

Vrekoussis, M., Wittrock, F., Richter, A., and Burrows, J. P.: Temporal and spatial variability of glyoxal as observed from space, Atmos. Chem. Phys., 9, 4485-4504, 10.5194/acp-9-4485-2009, 2009.

Wang, X., Gong, P., Sheng, J., Joswiak, D. R., and Yao, T.: Long-range atmospheric transport of particulate Polycyclic Aromatic Hydrocarbons and the incursion of aerosols to the southeast Tibetan Plateau, Atmospheric Environment, 115, 124-131, http://dx.doi.org/10.1016/j.atmosenv.2015.04.050, 2015.

Wang, Y., Choi, Y., Zeng, T., Ridley, B., Blake, N., Blake, D., and Flocke, F.: Late-spring increase of trans-Pacific pollution transport in the upper troposphere, Geophysical Research Letters, 33, n/a-n/a, 10.1029/2005GL024975, 2006.

Wang, Y., Choi, Y., Zeng, T., Davis, D., Buhr, M., Gregory Huey, L., and Neff, W.: Assessing the photochemical impact of snow emissions over Antarctica during ANTCI 2003, Atmospheric Environment, 41, 3944-3958, http://dx.doi.org/10.1016/j.atmosenv.2007.01.056, 2007.Wittrock, F., Richter, A., Oetjen, H., Burrows, J. P., Kanakidou, M., Myriokefalitakis, S., Volkamer, R., Beirle, S., Platt, U., and Wagner, T.: Simultaneous global observations of glyoxal and formaldehyde from space, Geophysical Research Letters, 33, 5, 10.1029/2006gl026310, 2006.

Xu, B., Cao, J., Hansen, J., Yao, T., Joswia, D. R., Wang, N., Wu, G., Wang, M., Zhao, H., Yang, W., Liu, X., and He, J.: Black soot and the survival of Tibetan glaciers, Proceedings of the National Academy of Sciences, 106, 22114-22118, 10.1073/pnas.0910444106, 2009.

Yang, Q., Wang, Y., Zhao, C., Liu, Z., Gustafson, W. I., and Shao, M.: NOx Emission Reduction and its Effects on Ozone during the 2008 Olympic Games, Environmental Science & Technology, 45, 6404-6410, 10.1021/es200675v, 2011.

Yao, T., Wang, Y., Liu, S., Pu, J., Shen, Y., and Lu, A.: Recent glacial retreat in High Asia in China and its impact on water resource in Northwest China, Science in China Series D: Earth Sciences, 47, 1065-1075, 10.1360/03yd0256, 2004.

Zeng, T., Wang, Y., Chance, K., Browell, E. V., Ridley, B. A., and Atlas, E. L.: Widespread persistent near-surface ozone depletion at northern high latitudes in spring, Geophysical Research Letters, 30, 2298, 10.1029/2003GL018587, 2003.

Zeng, T., Wang, Y., Chance, K., Blake, N., Blake, D., and Ridley, B.: Halogen-driven low-altitude O3 and hydrocarbon losses in spring at northern high latitudes, Journal of Geophysical Research: Atmospheres, 111, D17313, 10.1029/2005JD006706, 2006.

Zhang, Q., Streets, D. G., Carmichael, G. R., He, K. B., Huo, H., Kannari, A., Klimont, Z., Park, I. S., Reddy, S., Fu, J. S., Chen, D., Duan, L., Lei, Y., Wang, L. T., and Yao, Z. L.: Asian emissions in 2006 for the NASA INTEX-B mission, Atmos. Chem. Phys., 9, 5131-5153, 10.5194/acp-9-5131-2009, 2009.

Zhang, R., Wang, H., Qian, Y., Rasch, P. J., Easter, R. C., Ma, P. L., Singh, B., Huang, J., and Fu, Q.: Quantifying sources, transport, deposition, and radiative forcing of black carbon over the Himalayas and Tibetan Plateau, Atmos. Chem. Phys., 15, 6205-6223, 10.5194/acp-15-6205-2015, 2015.

Zhang, Y., Wang, X., Blake, D. R., Li, L., Zhang, Z., Wang, S., Guo, H., Lee, F. S., Gao, B., and Chan, L.: Aromatic hydrocarbons as ozone precursors before and after outbreak of the 2008 financial crisis in the Pearl River Delta region, south China, Journal of geophysical research: atmospheres, 117, 2012.

Zhang, Y., Wang, Y., Gray, B. A., Gu, D., Mauldin, L., Cantrell, C., and Bandy, A.: Surface and free tropospheric sources of methanesulfonic acid over the tropical Pacific Ocean, Geophysical Research Letters, 41, 2014GL060934, 10.1002/2014GL060934, 2014.

Zhang, Y., and Wang, Y.: Climate-driven ground-level ozone extreme in the fall over the Southeast United States, Proceedings of the National Academy of Sciences, 113, 10025-10030, 10.1073/pnas.1602563113, 2016.

Zhang, Y., Wang, Y., Chen, G., Smeltzer, C., Crawford, J., Olson, J., Szykman, J., Weinheimer, A. J., Knapp, D. J., Montzka, D. D., Wisthaler, A., Mikoviny, T., Fried, A., and Diskin, G.: Large vertical gradient of reactive nitrogen oxides in the boundary layer: Modeling analysis of DISCOVER-AQ 2011 observations, Journal of Geophysical Research: Atmospheres, 121, 1922-1934, 10.1002/2015JD024203, 2016.

Zhao, C., and Wang, Y.: Assimilated inversion of NOx emissions over east Asia using OMI NO2 column measurements, Geophysical Research Letters, 36, L06805, 10.1029/2008GL037123, 2009.

Zhao, C., Wang, Y., Choi, Y., and Zeng, T.: Summertime impact of convective transport and lightning NOx production over North America: modeling dependence on meteorological simulations, Atmos. Chem. Phys., 9, 4315-4327, 10.5194/acp-9-4315-2009, 2009a.

Zhao, C., Wang, Y., and Zeng, T.: East China Plains: A "Basin" of Ozone Pollution, Environmental Science & Technology, 43, 1911-1915, 10.1021/es8027764, 2009b.

Zhao, C., Wang, Y., Yang, Q., Fu, R., Cunnold, D., and Choi, Y.: Impact of East Asian summer monsoon on the air quality over China: View from space, Journal of Geophysical Research: Atmospheres, 115, D09301, 10.1029/2009JD012745, 2010.

20

Atmospheric
Chemistry
and Physics
Discussions

Open Access

EGU
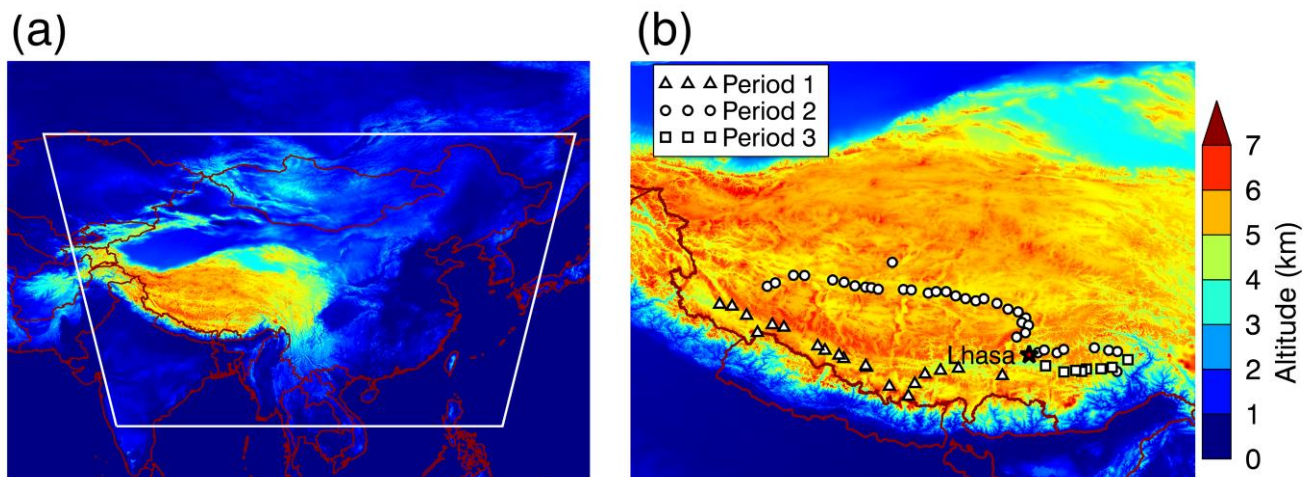
Figure 1: Overview of regions involved in this study. White polygon in (a) represents the domain margin of the model. Locations of observations for Period 1 (Oct 13-17, 2010, triangle), Period 2 (Oct 19-24, 2010, circle) and Period 3 (Oct 25, 2010, square) are shown in (b). Altitude data from Global Topographic Data (GTOPO30, courtesy of the U.S. Geological Survey) is shown as colored background.
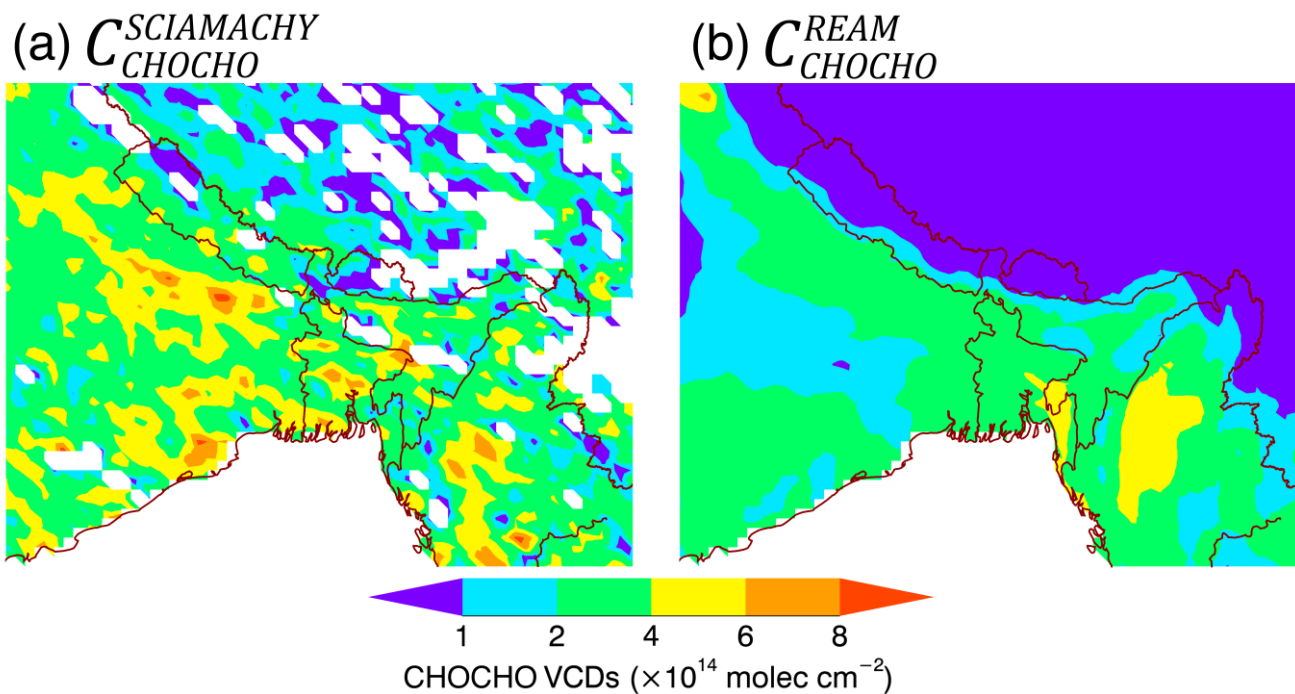
Figure 2: SCIAMACHY observed (a) and REAM simulated (b) CHOCHO VCDs for October 2010. White areas in the observations denote missing data or ocean.

5

Atmospheric
Chemistry
and Physics
Discussions
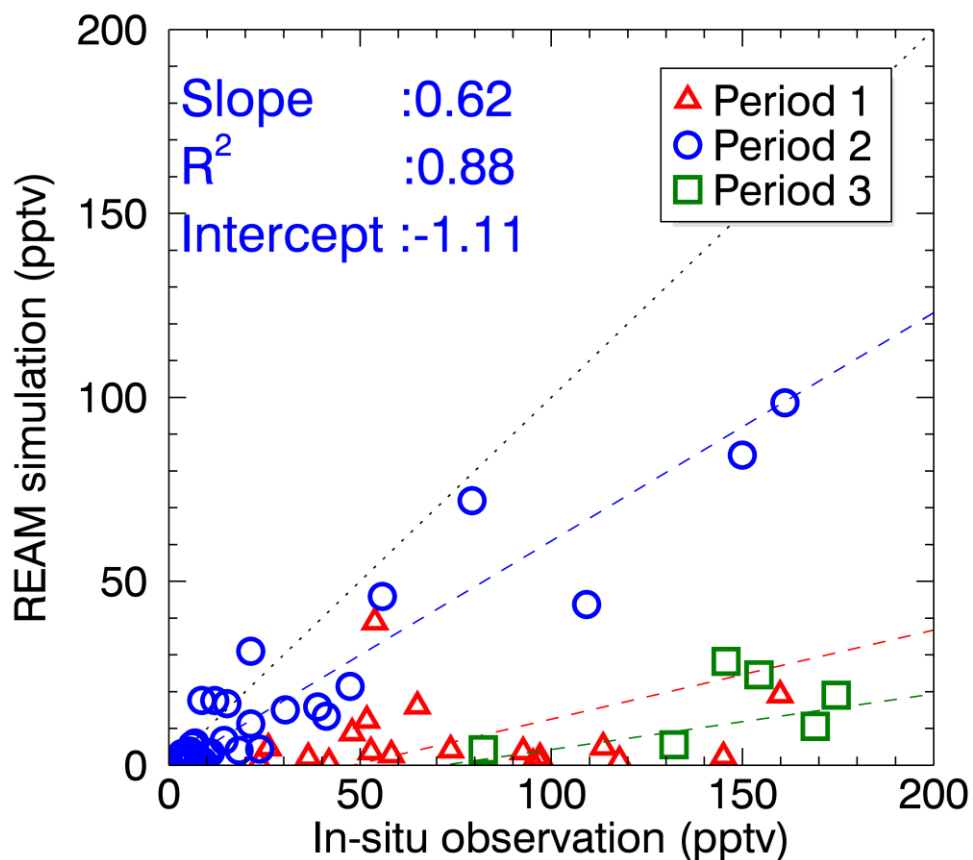
Figure 3: Comparison between REAM simulated reactive aromatics concentrations (Y-axis) and in situ observations (X-axis). REAM results are archived corresponding to the time and location of the observations. Linear regression results for three periods are shown in red (slope=0.24, R²=0.00), blue (slope=0.62, R²=0.88), and green (slope=0.15, R²=0.02) dashed lines, respectively.

5
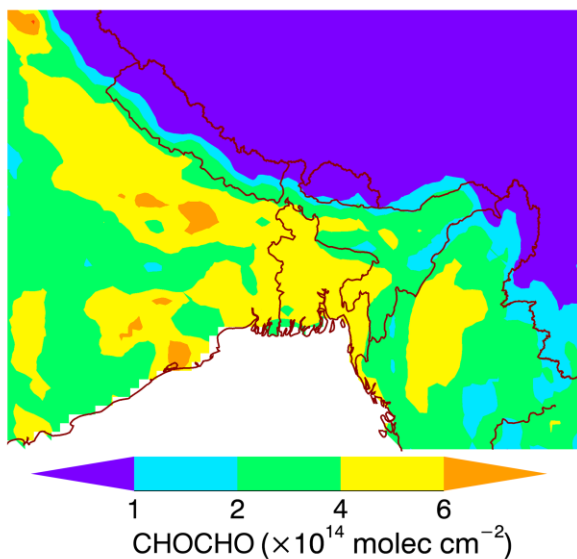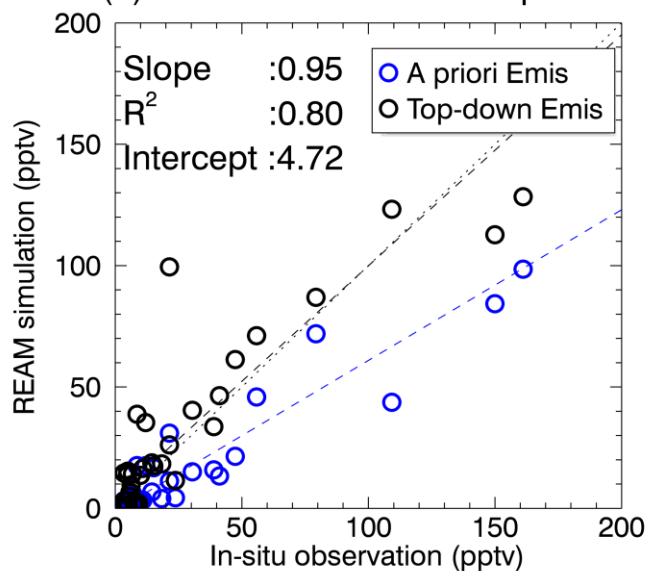
Figure 4: REAM simulated CHOCHO VCDs with top-down emissions (a) and comparison of simulated and observed reactive aromatics concentrations during Period 2 (b). Blue and black circles in panel (b) represent REAM simulation with a priori (slope=0.62, R^2=0.88) and with top-down (slope=0.95, R^2=0.80) emissions, respectively.
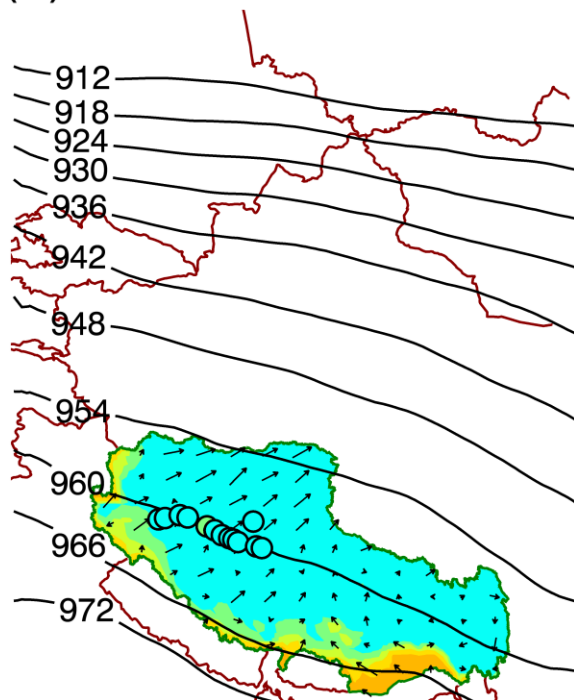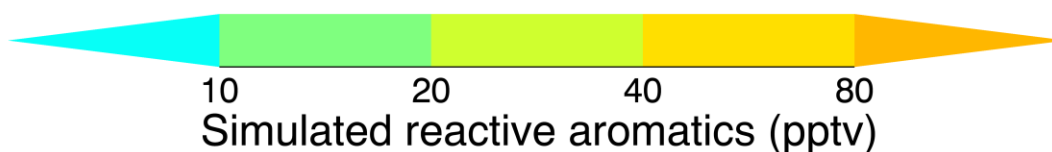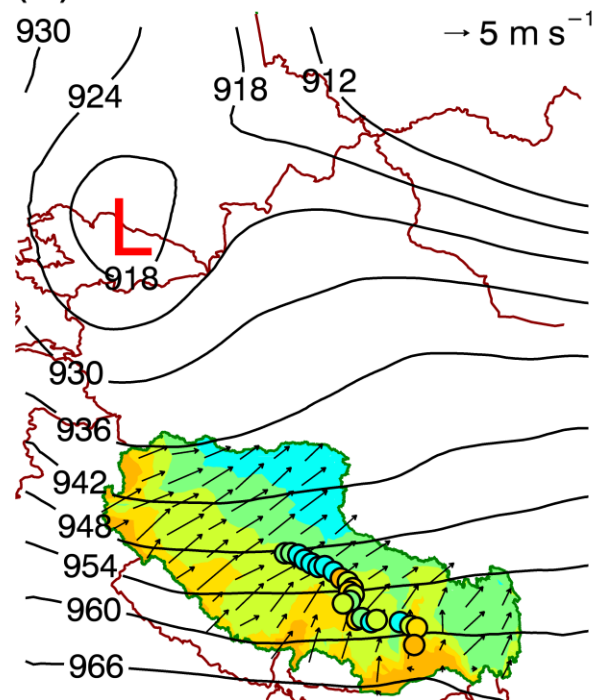
5

Figure 5: Distributions of surface wind and concentrations of reactive aromatics over the Tibetan Plateau during October 19-20, 2010 (a) and October 21-24, 2010 (b). Circles show the observed reactive aromatics concentrations. Composite distributions of simulated reactive aromatics concentrations and surface wind over Tibet, corresponding to sampling time of the observations, are shown in color and by arrows, respectively. Corresponding 300 hPa geopotential height fields are shown by contour lines. The border of Tibet Autonomous Region is colored green.

Figure 6: Reactive aromatics emitted from Tibet (red), India and nearby regions ("South Asia", blue) and China excluding Tibet ('China w/o Tibet', green) corresponding to in situ observations in the REAM simulation with top-down emissions. Contributions from the other regions are negligible.

5

Atmospheric
Chemistry
and Physics

Open Access

EGU

Discussions
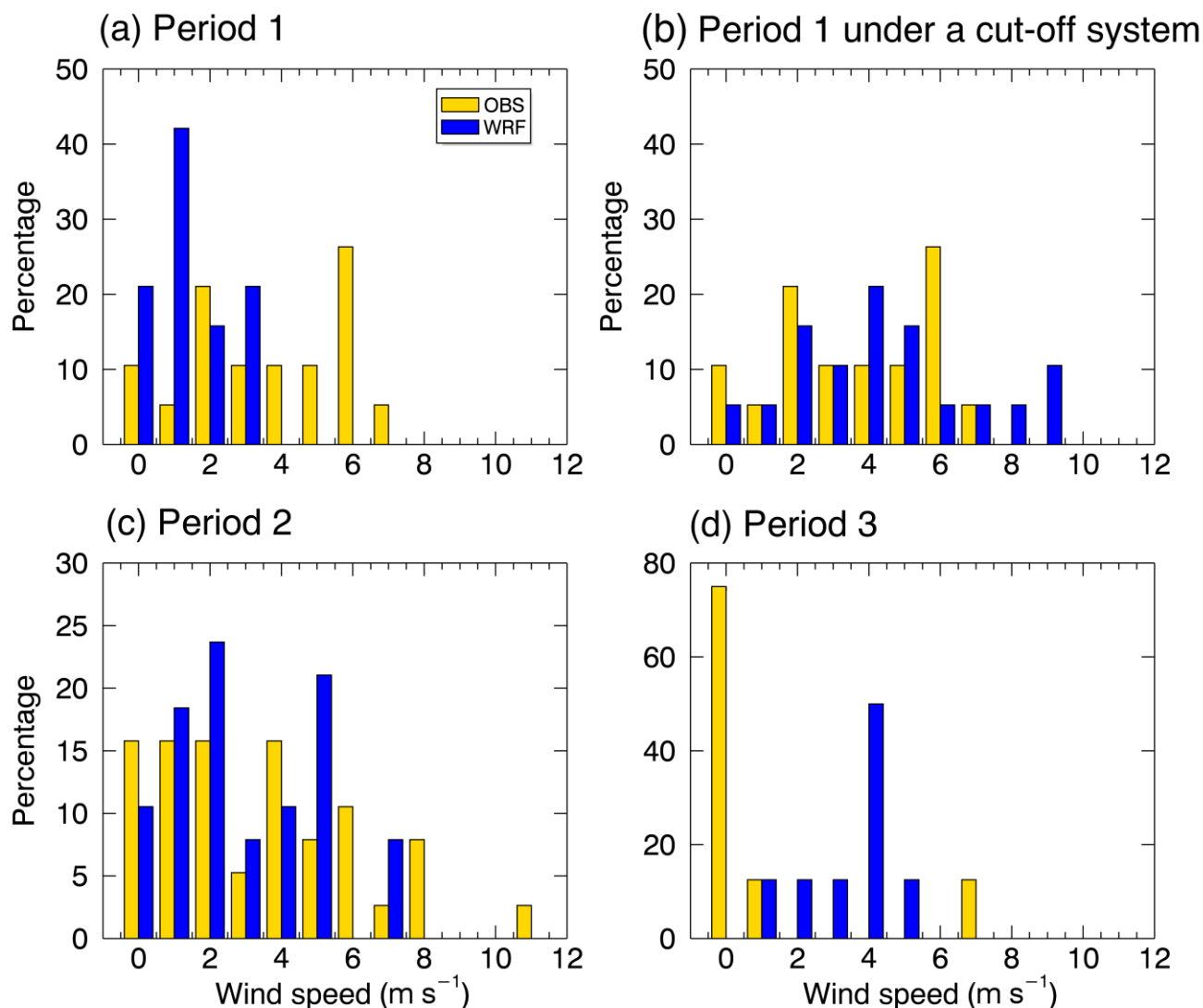
Figure 7: Histograms of observed and simulated wind speed for Period 1 (a), Period 2 (c) and Period 3 (d). Panel (b) shows the wind histogram of October 23 with an upper tropospheric cut off low system. Model results are sampled at the same time and location as the observations. In Panel (d), the date information is not used. Wind speed is binned at 1 m/s interval.

5
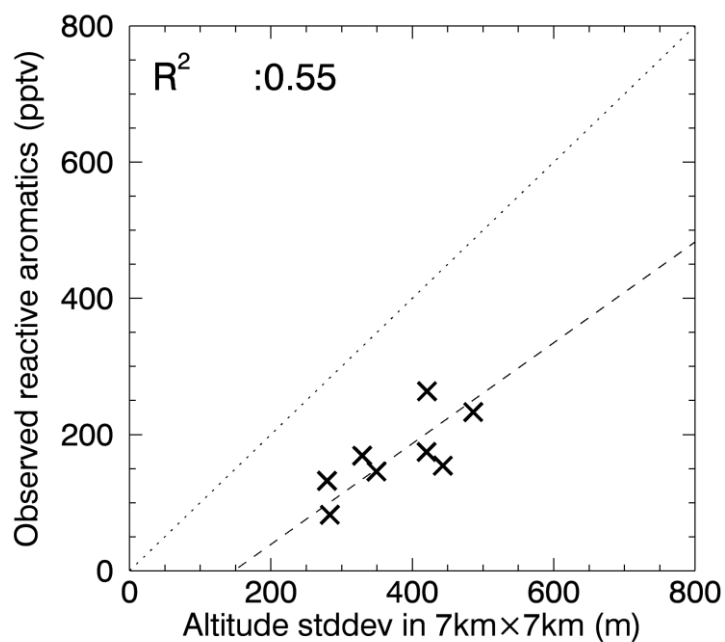
Figure 8: Observed reactive aromatics as a function of terrain complex during Period 3. The latter is computed as the standard deviation of altitude in a 7km x 7km region centered at the sampling location. The dash line denotes a least-squares regression.